

Distribution of deep-water scleractinian and stylasterid corals across abiotic environmental gradients on three seamounts in the Anegada Passage

Steven R Auscavitch $^{\text{Corresp., 1}}$, Jay J Lunden $^{\text{1}}$, Alexandria Barkman $^{\text{1}}$, Andrea M Quattrini $^{\text{2}}$, Amanda W J Demopoulos $^{\text{3}}$, Erik E Cordes $^{\text{1}}$

Corresponding Author: Steven R Auscavitch Email address: steven.auscavitch@temple.edu

In the Caribbean Basin, the distribution and diversity patterns of deep-sea scleractinian corals and stylasterid hydrocorals are poorly known compared to their shallow water relatives. In this study, we examined species distribution and community assembly patterns of scleractinian and stylasterid corals on three high-profile seamounts within the Anegada Passage, a deep-water throughway linking the Caribbean Sea and western North Atlantic. Using remotely operated vehicle surveys conducted on the E/V Nautilus by the ROV Hercules in 2014, we characterized coral assemblages and seawater environmental variables between 162-2157 m on Dog Seamount, Conrad Seamount, and Noroît Seamount. In all, 13 morphospecies of scleractinian and stylasterid corals were identified from video with stylasterids being numerically more abundant than both colonial and solitary scleractinians. Cosmopolitan framework-forming species including Madrepora oculata and Solenosmilia variabilis were present but occurred in patchy distributions among the three seamounts. Framework-forming species occurred at or above the depth of the aragonite saturation horizon with stylasterid hydrocorals being the only coral taxon observed below Ω_{arag} values of 1. Coral assemblage variation was found to be strongly associated with depth and aragonite saturation state, while other environmental variables exerted less influence. This study enhances our understanding of the factors that regulate scleractinian and stylasterid coral distribution in an underreported marginal sea and establishes a baseline for monitoring future environmental changes due to ocean acidification and deoxygenation in the tropical western Atlantic.

¹ Department of Biology, Temple University, Philadelphia, PA, USA

² National Museum of Natural History, Smithsonian Institution, Washington, D.C., United States

³ Wetland and Aquatric Research Center, US Geological Survey, Gainesville, Florida, USA



Distribution of deep-water scleractinian and stylasterid corals across abiotic environmental

3 gradients on three seamounts in the Anegada

4 Passage

5

Steven R. Auscavitch¹, Jay J. Lunden¹, Alexandria Barkman¹, Andrea M. Quattrini², Amanda W.
 J. Demopoulos³, Erik E. Cordes¹

8

- ¹ Department of Biology, Temple University, Philadelphia, PA, USA.
- 10 ² National Museum of Natural History, Smithsonian Institution, Washington, DC. USA.
 - ³ Wetland and Aquatic Research Center, U.S. Geological Survey, Gainesville, FL, USA.

11 12

- 13 Corresponding Author:
- 14 Steven R. Auscavitch¹
- 15 steven.auscavitch@temple.edu
- 16 1900 N 12th St. Philadelphia, PA, 19122, USA.

17 18

Abstract

19 20

21

22

23

24

25

26

27

28

29

30

31

In the Caribbean Basin, the distribution and diversity patterns of deep-sea scleractinian corals and stylasterid hydrocorals are poorly known compared to their shallow water relatives. In this study, we examined species distribution and community assembly patterns of scleractinian and stylasterid corals on three high-profile seamounts within the Anegada Passage, a deep-water throughway linking the Caribbean Sea and western North Atlantic. Using remotely operated vehicle surveys conducted on the E/V *Nautilus* by the ROV *Hercules* in 2014, we characterized coral assemblages and seawater environmental variables between 162-2157 m on Dog Seamount, Conrad Seamount, and Noroît Seamount. In all, 13 morphospecies of scleractinian and stylasterid corals were identified from video with stylasterids being numerically more abundant than both colonial and solitary scleractinians. Cosmopolitan framework-forming species including *Madrepora oculata* and *Solenosmilia variabilis* were present but occurred in patchy



distributions among the three seamounts. Framework-forming species occurred at or above the depth of the aragonite saturation horizon with stylasterid hydrocorals being the only coral taxon observed below Ω_{arag} values of 1. Coral assemblage variation was found to be strongly associated with depth and aragonite saturation state, while other environmental variables exerted less influence. This study enhances our understanding of the factors that regulate scleractinian and stylasterid coral distribution in an underreported marginal sea and establishes a baseline for monitoring future environmental changes due to ocean acidification and deoxygenation in the tropical western Atlantic.

Introduction

Global and regional modelling efforts in parallel with observational studies have contributed to our understanding of the distribution of framework-forming azooxanthellate corals in the deep sea (>200 m depth). However, a significant number of data deficient localities persist, most often hindered by a lack of records from direct seafloor observation and *in situ* environmental data. A number of environmental variables have been observed to control the distribution of deep-water azooxanthellate scleractinian corals and stylasterid hydrocorals, including parameters linked to depth, terrain, hydrography, and seawater chemistry (Guinotte et al., 2006; Cairns, 2007; Davies & Guinotte, 2011). In the tropical western Atlantic, a center for deep-water scleractinian diversity (Cairns, 2007), additional direct observational data are needed to validate modelling efforts.

The growth of a scleractinian coral colony and formation of the aragonitic calcium carbonate skeleton are generally dependent upon the ambient seawater aragonite saturation state

 (Ω_{arag}) being greater than 1, or supersaturated. However, some deep-water scleractinian corals,



including the cosmopolitan species Solenosmilia variabilis and Enallopsammia rostrata, have
been reported well below the saturation horizon (the depth at which Ω_{arag} = 1) on the Tasmanian
Seamounts (Thresher et al., 2011). A more recent survey of seamounts in the Northwestern
Hawaiian Islands and Emperor Seamounts documented living colonial scleractinian reefs at Ω_{arag}
as low as 0.71 (Baco et al., 2017). Previous studies lend support for targeted observational
surveys in underexplored regions in order to delineate species distribution patterns with respect
to aragonite saturation and other environmental variables. These efforts are particularly salient in
light of potential and ongoing anthropogenic impacts to deep-sea coral ecosystems (Ragnarsson
et al., 2017), including global climate change and ocean acidification (Gleckler et al., 2016;
Pérez et al., 2018), deep-water drilling and resource extraction (Cordes et al., 2016), bottom-
contact fishing (Watling & Norse, 1998), and deep-sea crust mining (Miller et al., 2018).
The Greater-Lesser Antilles transition zone is one of the most sparsely surveyed yet
biogeographically important deep-water entries from the western Atlantic Ocean into the
Caribbean Basin. Topographic features, such as seamounts and other submarine banks associated
with deformation along tectonic plate boundaries, are important contributors to the
environmental complexity of the deep-sea benthos. In the Anegada Passage, Dog Seamount,
Conrad Seamount, Noroît Seamount, and Barracuda Bank are some of the most prominent of the
large (> 2km in neight above the surrounding seafloor) seamounts and banks present, ranging
from abyssal to mesophotic depths. Typical environmental characteristics of seamounts,
including substrate heterogeneity, enhanced productivity and carbon flux, and variable currents
(Rogers, 2018), create the potential for deep-water biodiversity hotspots in the region and
elevated species abundance relative to the adjacent continental margins and slopes. Previous
studies indicate that at depths > 200 m, azooxanthellate corals generally prefer hard substrata that



78	exhibit topographic complexity (Roberts et al., 2009; Georgian, Shedd & Cordes, 2014). As
79	such, seamounts are one example of topographically complex deep-water features that provide
80	ideal hard substrate for corals (Rogers, 1994). Yet very few seamount benthic communities in the
81	Caribbean region have been characterized with respect to these important abiotic gradients.
82	Throughout the tropical western Atlantic, scleractinian species diversity and distributions
83	are relatively well-known from shallow waters but the extent of their distribution below 150 m is
84	poorly understood. For deep-water azooxanthellate corals, 81 species have been reported at
85	depths greater than 50 m for the Greater and Lesser Antilles (Cairns, 2007). As with
86	scleractinians, stylasterid hydrocorals are reportedly diverse from the Lesser Antilles (Cairns,
87	1986), can occur in high densities in the tropical western Atlantic (Messing, Neumann & Lang,
88	1990), and are composed of rigid, primarily aragonitic coralla (Cairns & Macintyre, 1992).
89	Additionally, three-dimensional structures produced by deep-water stylasterids provide habitat
90	for fishes (Love, Lenarz & Snook, 2010) and invertebrate fauna (Braga-Henriques et al., 2011;
91	Reed et al., 2013). Efforts have also been made to understand the biogeographic context of
92	Caribbean ecoregions using deep-water corals in order to support conservation strategies (Cairns
93	& Chapman, 2001; Miloslavich et al., 2010; Hernández-Ávila, 2014). In the Caribbean Basin,
94	patterns in deep-sea coral beta diversity (e.g., species turnover) between ecoregions have been
95	attributed to topography and oceanography (Hernández-Ávila, 2014). Within the insular
96	Caribbean, the Greater Antilles and Lesser Antilles regions are found to diverge into two
97	ecoregions, one encompassing the Greater Antilles islands and the other the Lesser Antilles
98	islands, at continental slope depths (200-2000 m) (Hernández-Ávila, 2014). At larger
99	biogeographic scales and evolutionary time, deep-water currents or water masses have been
100	hypothesized as distribution pathways for constraining cosmopolitan habitat-forming corals like



Lophelia pertusa in the western Atlantic (Arantes et al., 2009; Henry, 2011). While widespread seamount surveys from the Caribbean Basin remain rare, the effect of environmental variables like temperature, dissolved oxygen, and water mass has been demonstrated for demersal fishes on seamounts in the Anegada Passage (Quattrini et al., 2017).

The present study focuses on describing patterns in the distribution of deep-water scleractinians and stylasterid corals on three prominent seamounts in the northeastern Caribbean Sea. In addition to the primary abiotic oceanographic variables including temperature, salinity, and dissolved oxygen, we explore the distribution of aragonitic corals in the region with respect to the aragonite saturation state in this region of the western Atlantic Ocean. As a suspected driver of change in deep-water coral community structure, we also examine the relationship between water mass structure and community similarity in the bathyal zone, hypothesizing that different water masses would have distinct coral assemblages. Finally, we aim to identify abiotic oceanographic variables that most strongly influence the presence of hard corals and their contribution to changes in community similarity for this locality.

Materials & Methods

ROV Surveys

This study examined sites within the Anegada Passage in the northeastern corner of the Caribbean Sea (Fig. 1). Three seamounts of varying summit depths were surveyed in September 2014 using the ROV *Hercules* during E/V *Nautilus* cruise NA052 (Table 1). Three dives were conducted on Dog Seamount (276 to 1035 m depth), two were conducted on Conrad Seamount (162 to 1314 m depth), and two were conducted on Noroît Seamount (949 to 2206 m depth).





Efforts were made to cover similar depth ranges on each feature for direct comparison as permitted by the bathymetry.

The ROV was deployed to a maximum target depth on each seamount and generally moved to shallower depths up slope. The ROV continuously traversed the seafloor as near to the bottom as practical at a slow, steady speed (~0.1-0.2 knots, ~0.1 m/s); however, transects were occasionally interrupted by stopping the ROV for sampling and detailed camera zooms. The ROV was equipped with a high-definition camera and paired scaling lasers (10 cm apart). During the dives, the forward-facing cameras were set on wide-angle view, but frequent snap-zooms (up to 20 sec) were conducted to aid in species identification. The ROV was also equipped with a Seabird FastCAT 49 conductivity-temperature-depth (CTD) logger and an Aanderaa oxygen optode to measure dissolved oxygen (DO). The ROV was tracked on the seafloor using an ultrashort baseline (USBL) tracking system as well as a Doppler Velocity Log (DVLNAV).

Seawater Collection and Carbonate Chemistry Analysis

Seawater samples (n = 34) were collected both in the water column and at the benthos using Niskin bottles mounted to the ROV *Hercules* (Supplementary Table 1). On bottom, seawater samples were collected within 1-2 meters of the benthos and usually co-occurred with the observation of scleractinian colonies on the seafloor. For all seawater samples, co-located physical data (pressure, temperature, salinity, and oxygen) were obtained using vehicle mounted conductivity-temperature-depth (Paroscientific Digiquartz, SBE 49Plus) and oxygen (Aanderaa Optode 3830) sensors, respectively. Upon recovery of the ROV, samples were immediately transferred to 500 mL high-density polyethylene (HDPE) containers according to Best Practices for Ocean CO₂ measurements (Dickson, Sabine & Christian, 2007). While HDPE containers are



suitable for long-term storage of seawater for total alkalinity analyses (Huang, Wang & Cai, 2012), they are not suitable for long-term storage for pH or dissolved inorganic carbon analyses as they are permeable to CO_2 . Accordingly, pH was measured within 1 hour of collection onboard the vessel. Immediately following pH measurement, samples were poisoned with 100 μ L saturated mercuric chloride solution and stored in a cool, dark location. Total alkalinity was measured in the laboratory in triplicate according to methods previously described (Lunden, Georgian & Cordes, 2013; Georgian et al., 2016a), and final Ω_{arag} values were computed using CO2calc (Robbins et al., 2010). Due to the logistical challenge of pairing a discrete water sample with each individual scleractinian coral observation, we generated a predictive model to interpolate Ω_{arag} at the depth of each coral observation based on temperature, dissolved oxygen, and salinity (for methodology see Georgian et al., 2016a).

ROV video analysis

Colonial and solitary coral occurrences were documented using high-definition video transects during each of the ROV dives. Video segments where collections occurred, where the vehicle was too high off the bottom, moving backwards, or of generally poor quality, were removed from analysis. For the purpose of this analysis, we defined structure-forming corals as colonial members of the Scleractinia and hydrozoan family Stylasteridae. Consistent morphospecies identifications were used throughout the analyses. Voucher specimens for morphological identification were obtained using the ROV platform. If necessary, further identifications of coral species were made using taxonomic keys and assistance from taxonomic specialists. Colony height was measured, where possible, by referencing scaling lasers. Individuals or colonies above a 5-cm height threshold were typically identifiable based on laser



scalers. If occurrences could not be readily identified below the 5-cm threshold, they were omitted from analysis. Each observation was paired with an associated time-stamp for reference to *in situ* environmental data (temperature, depth, dissolved oxygen concentration, and salinity) collected by ROV CTD and oxygen optode sensors.

174175

170

171

172

173

Community Analyses

176177

178

179

180

181

182

183

184

185

186

187

188

189

190

191

192

193

194

Sampling effort was evaluated for seamounts individually and for all seamounts combined by sample-based species accumulation curves. In order to assess community relationships among hard-coral assemblages, species abundance values (number of colonies or individuals for each species) were binned into 100 m depth segments for each seamount transect resulting in 28 total samples. Community-level analyses were conducted using standardized and 4th root transformed species abundance data in PRIMER v7 with PERMANOVA add-on (Clarke & Gorley, 2006; Anderson, Gorley & Clarke, 2008). Transformed and standardized species abundances were compiled into a Bray-Curtis resemblance matrix for further analyses. In order to test for significant differences among hard coral assemblages on different seamounts, a one-way analysis of similarity (ANOSIM) was conducted between features as well as between local water masses. Non-metric multidimensional scaling ordinations (nMDS) were conducted across all 28 samples. nMDS plots were overlaid with similarity profile (SIMPROF) analysis to show significant groupings of samples at the 95% level or greater (Clarke, Somerfield & Gorley, 2008). Similarity percentage (SIMPER) tests were used to identify taxa that contributed disproportionately to assemblage similarities within and between seamounts and water masses. Multivariate analyses were also used to explore the abiotic variables relevant to the variation observed in the coral assemblages. Environmental data for temperature, salinity, dissolved

oxygen, and Ω_{arag} were obtained from the calculated mean in each 100 m depth segment within



every transect. The mean was then 4th-root transformed and normalized within each variable. The BEST (BIO-ENV) routine (Clarke, Somerfield & Gorley, 2008) was applied to the dataset to determine which environmental variables would be useful predictor variables. A distance-based linear model (DistLM) with Akaike information criterion (AIC) was applied using the PERMANOVA add-on in PRIMER v7 (Anderson, Gorley & Clarke, 2008). Visualizations of the resemblance matrix with predictor variables were observed using a dbRDA (distance-based redundancy analysis) ordination with DistLM overlay.

Results

Survey Summaries

A total of 106 hours of bottom time was assessed across 7 dives (Table 1). Video records were annotated between the depth range of 162-2157 m. In all, 264 observations of solitary and framework-forming scleractinian corals and stylasterid hydrocorals were made across all three seamounts (Table 2). Three dives at Dog Seamount yielded 64 records from 284-849 m. From Conrad Seamount, 182 records were made from 166m to 1230 m across 2 dives. The deepest two dives at Noroît Seamount had 18 records reported from 1014-1626 m. Stylasterids made up the majority (53%) of coral observations, however most were observed at depths shallower than 400 m (Table 2). The majority of scleractinians observed were colonial, framework-forming species (100 colonies observed) while only 22 observations were made of solitary coral species, as they were often on or below the threshold for identification. For this reason, abundances of solitary scleractinians represent a minimum value. No scleractinians or stylasterids above the 5 cm size threshold were observed deeper than 1626 m on any seamount.

PeerJ

219220221	Water Mass Structure
222	Downcast CTD profiles from the ROV sensors were plotted and assessed at each seamount
223	using Ocean Data View v5 (Schlitzer, 2019). Profiles for each seamount were combined to create
224	one consensus profile for the Anegada Passage (Fig. 2). Water masses were identified following
225	published records of temperature, salinity, and dissolved oxygen profiles for the northeast
226	Caribbean and Anegada Passage; these include Subtropical Underwater (SUW) 100-200 m,
227	Sargasso Sea Water (SSW) 200-400 m, Tropical Atlantic Central Water (TACW) 400-700 m,
228	Antarctic Intermediate Water (AAIW) 700-1200 m, and North Atlantic Deep Water (NADW)
229	(>1200 m) (Morrison & Nowlin, 1982; Liu & Tanhua, 2019).
230	
231	Carbonate chemistry analysis
232	Water samples for carbonate chemistry analyses were collected at depth from 50 m to
233	2170 m. Total alkalinity ranged from 2291.4 to 2405.9 μmol·kg ⁻¹ , and pH ranged from 7.83 to
234	8.11, with minimum pH observed at 795 m depth. Measured Ω_{arag} values from Niskin bottle
235	collections ranged from 4.13 at 50 m depth to 0.99 at 2170 m depth. The aragonite saturation
236	state of the water column was modelled according to the following equation: $\Omega_{arag} = (T x)$
237	0.11407018) + (O x 0.00302922) + (S x 0.18168448) – 6.5216044 (stepwise backward
238	regression, $R^2 = 0.9857$, $p < 0.001$) where $T =$ temperature in °C, $O =$ oxygen concentration in
239	μ mol·L ⁻¹ , and S = salinity in parts per thousand (ppt). From this, predicted $Ω$ _{arag} values ranged
240	from 4.11 to 1.05, with highest value at 51 m at Dog Seamount and lowest value at 2195 m at
241	Noroît Seamount.
242	
243	Coral species Distribution Patterns



The single most abundant scleractinian coral species was *Solenosmilia variabilis* (44 colonies), but it was only observed on Conrad Seamount in a relatively narrow depth range, 409-569 m. Many structure-forming colonies were found to be associated with boulder and low, outcropping, hard rock substrate. This was followed by the more widespread *Madrepora oculata* (22 colonies), which occurred between 784 and 1540 m on all seamounts (Fig. 3). *Madrepora oculata*, which displayed two different growth forms from thin and sparsely branching to thick, robust colonies, possessed the widest depth distribution range for any colonial scleractinian coral. The deepest solitary scleractinian coral, *Javania cailleti*, was observed at 1626 m; this occurrence corresponds with one of the lowest measured Ω_{arag} values of 1.01.

The upper bathyal depths, shallower than 700 m, contained species with narrower depth distributions than those at lower bathyal depths (>800 m) (Fig. 3). The sub-700 m assemblage was composed of three species of scleractinians (*E. rostrata*, *M. oculata*, and *J. cailleti*) and one stylasterid (*Crypthelia* sp. 1). The shallowest depths, usually coinciding with the seamount summit, were dominated by two species of stylasterids, *Stylaster* sp. 1 and *Stylaster* cf. *duchassaingi*, as well as one azooxanthellate scleractinian, *Madracis myriaster*. On Conrad Seamount, pink and purple coralline algal crusts were observed as deep as 256 m depth and continued to be observed through shallower depths dominated by sponges, stylasterids, and black corals.

The majority of stylasterid species were restricted to depths less than 400 m with only *Crypthelia* exhibiting a wider depth distribution (Fig. 3). Only three morphospecies of stylasterids were large enough to be consistently identified during video annotation. Other unidentifiable stylasterids were combined into a fourth group, Stylasteridae spp. and shown for





reference. The most abundant species, *Stylaster* sp. 1, was found in a narrow depth range
 between 166-174 m on the summit of Conrad Seamount.
 Patterns of Coral Occurrences with Aragonite Saturation State

Measured Ω_{arag} values from water collected adjacent to corals were not significantly different (t-test, N=9, t=-0.23341, p=0.818) compared to what was calculated using the modelled aragonite saturation state data (Supplementary Fig. 1). All paired water samplings adjacent to coral observations occurred at or above the aragonite saturation horizon ($\Omega_{arag} > 1$) (Table 3). Multiple water samples for a single species were collected for only *M. oculata*. A full table of all 34 Niskin water bottle measurements and matched environmental variables is provided (Supplementary Table 1).

Using predicted values derived from CTD and sensor data on temperature, oxygen concentration, and salinity, all scleractinian and stylasterid corals were observed at $\Omega_{\rm arag}$ values of 0.99 to 3.45 (Fig. 4). For scleractinians, *Javania cailleti* occurred across the largest aragonite saturation state range, between 1.01 and 1.77. Among the Stylasteridae, *Crypthelia* sp. 1 occurred across the greatest range of saturation states from as low as 0.99 up to 2.83. Only three species were observed at or around the aragonite saturation horizon based on predicted saturation state values, *Crypthelia* sp. 1 ($\Omega_{\rm arag}$ =0.99), *M. oculata* ($\Omega_{\rm arag}$ =1.00) and *J. cailleti* ($\Omega_{\rm arag}$ =1.01).

Community Structure Patterns

Species-accumulation curves were evaluated for seamounts individually and in aggregate for all seamounts. Combined, all seamounts (100-1700 m) revealed a more complete sampling effort than among single seamount coral assemblages (Fig. 5). Individually, species accumulation



curves for Dog, Conrad, and Noroît seamounts were not asymptotic, and therefore are likely to 290 accumulate additional coral species with increased sampling effort. 291 Analysis of similarity (two-way nested, depth within seamount, Global R=0.122, p=0.05) conducted among seamounts revealed significant differences in coral assemblages between Dog 292 293 and Noroît Seamounts (R=0.544, p=0.006), but not Conrad and Dog seamounts (R=-0.001, 294 p=0.379) or Conrad and Noroît seamounts (R=0.029, p=0.292) (Supplementary Table 2). A one-295 way ANOSIM (Global R=0.464, p=0.001) between water masses revealed significant differences 296 in coral assemblages between SSW and TACW (R=0.46, p=0.003), AAIW (R=0.53, p=0.002), 297 and NADW (R=0.60, p=0.008) as well as between TACW and NADW (R=0.93, p=0.001) and AAIW and NADW (R=0.361, p=0.01) (Supplementary Table 3). 298 299 Non-metric multi-dimensional ordination with SIMPROF groupings revealed five statistically 300 significant groupings; two shallow assemblages composed of 100 m depth-binned samples from between 100-600 m and 200-400 m, two mid-depth assemblages (500-700 m and 700-1100 m), 301 302 and one deep assemblage (1100-1600 m) (Fig. 6). Outliers from these groupings occurred in the 600-700 m and 1100-1200 m depth bins on Conrad Seamount and between 1300-1400 m on 303 Noroît Seamount. Within SIMPROF groupings, the shallowest depth grouping showed the 304 305 greatest amount of dissimilarity among samples (a metric of beta diversity) among the three 306 seamounts while the lowest occurred in the deepest group. 307 Dog Seamount exhibited the lowest beta diversity of coral assemblages among all three 308 seamounts and the highest average similarity at 61% (one-way SIMPER analysis), with the average similarity between 100 m depth bins being most strongly influenced by Crypthelia sp. 309 310 1, which contributed to 96.6% of the relative abundance. Noroît Seamount had the second 311 highest similarity (38.2%), with M. oculata accounting for 84.7% of the similarity. Conrad



312	Seamount had the lowest average similarity (15%), with stylasterids Crypthelia sp. 1 and
313	Stylaster cf. duchassaingi being the greatest contributors to average similarity with 48.4% and
314	21.5%, respectively. Between seamounts, Noroît differed from Dog and Conrad, primarily due to
315	the higher abundance of <i>M. oculata</i> at Noroît Seamount. Noroît Seamount had nearly triple the
316	average abundance of <i>M. oculata</i> compared to Conrad Seamount. Conrad and Dog Seamounts
317	differed primarily due to the contribution of Crypthelia sp. 1 and M. myriaster, which were
318	present on Conrad at 2 to 3 times higher average abundance than at Dog Seamount.
319	Within water masses, the greatest average similarity of coral assemblages occurred within
320	NADW (54%) followed by TACW (51%) and finally SSW at (32 %). The abundance of
321	scleractinians was responsible for greater similarities within deep water masses (M. oculata and
322	Javania cailleti in NADW) while stylasterids were more commonly associated with driving
323	patterns of similarity within intermediate and shallower water masses (Crypthelia sp. 1 in
324	TACW, AAIW and Stylaster cf. duchassaingi in SSW). Between immediately adjacent water
325	masses, the greatest average dissimilarity was observed between SUW and SSW (92.3%) and the
326	lowest between TACW and AAIW (56.7%), indicating higher rates of turnover (beta diversity)
327	for shallower water masses than deeper ones.
328	Results from the BEST analysis indicated that the largest percentage of biological variation
329	was correlated with depth (r=0.536). The BEST routine also indicated that the greatest
330	correlation occurred with the four combined factors of depth, Ω_{arag} , temperature, and dissolved
331	oxygen (r=0.614). Sequential tests in the DistLM analysis indicated that depth (AIC=223.88,
332	p=0.001) and Ω_{arag} (AIC= 215.87, p=0.001) were the greatest explanatory variables influencing
333	coral assemblages on seamounts in the Anegada Passage. Temperature, salinity, and oxygen did
334	not explain a significant portion of the biological variation in this test. Redundancy analyses



resulted in 59.4% of the DistLM model variation explained by the primary axis (dbRDA1) and 32.6% explained by the second (dbRDA2) (Fig. 7). Likewise, the first axis explained 32.8% of the total biological variation observed and the second axis explained 18%. The primary axis was most closely correlated with oxygen (r = -0.82), while the second was most closely related to temperature (r = -0.61).

340

335

336

337

338

339

341

342

343

344

345

346

347

348

349

350

351

352

353

354

355

356

357

Discussion

Seamounts in the Anegada Passage were found to harbor communities of stony and lace corals throughout the bathyal depth range from summit depths as shallow as 166 m to a maximum of 1626 m. Both stylasterid and scleractinian coral species with aragonitic skeletons were largely present above the aragonite saturation horizon in this region of the western Atlantic Ocean, with the understanding that sampling effort below the ASH was limited to one transect at Noroît Seamount (Table 1). Nevertheless, we were able to identify the depth of the ASH as occurring between 2000-2200 m in the Anegada Passage (Supplementary Fig. 1), which is consistent with previous reports from the North Atlantic Ocean (Jiang et al., 2015). Only stylasterids in the genus Crypthelia were observed to occur below the aragonite saturation horizon ($\Omega_{arag} = 0.99$), but others, including the framework-forming species *Madrepora oculata*, occurred at saturation states as low as $\Omega_{arag} = 1.0$. However, it is likely that aragonitic corals live below the aragonite saturation horizon within our study region, as our sampling effort was lower at these depths. Also noteworthy was the observation of live crustose coralline algae at a depth of 256 m, which is comparable to the deepest known record from San Salvador Island (268 m) in The Bahamas (Littler et al., 1986).



Overlying water masses were a significant indicator of community assembly differences between SSW (Sargasso Sea Water) and deeper water masses, but not the shallowest water mass, Subtropical Underwater (SUW) and deeper strata of the water column. Oceanographic variables that most strongly influenced the presence of aragonitic corals and their contribution to changes in community similarity were depth and aragonite saturation state, with temperature, salinity, and dissolved oxygen making less significant contributions.

The tropical western Atlantic is a known diversity center for azooxanthellate scleractinian corals and stylasterid hydrocorals (Cairns, 2007, 2011). This study provides new distribution records for deep-water coral species in the northeastern Caribbean and builds on existing efforts to characterize the azooxanthellate coral fauna of the tropical western Atlantic (Cairns, 1979; Cairns & Chapman, 2001; Lutz & Ginsburg, 2007). Specifically, 7 species or morphospecies of stony corals within the genera *Javania*, *Madrepora*, *Madracis*, *Enallopsammia*, *Dendrophyllia*, and *Caryophyllia* have been added to local species inventories in the Anegada Passage (Fig. 8). New records from photographic and physical specimens aid in resolving the complex biogeography of the Greater-Lesser Antilles Transition zone seamounts with respect to the western North Atlantic (Supplementary Table 4). The paucity of records paired with environmental parameters from global biogeographic databases makes these observations critical to understanding the species distribution dynamics of marginal Atlantic seas and how coral distribution may be affected by future ocean climatic changes.

Stony coral assemblages in the Anegada Passage were similar to those observed in other parts of the western Atlantic Ocean with a few noteworthy absences. Absent from our records from the Anegada Passage seamounts include reef-forming species like *L. pertusa* and *E. profunda*, as well as cosmopolitan cup coral species like *Desmophyllum dianthus*, which are



reportedly more common throughout the U.S. southeast continental shelf and Gulf of Mexico (Schroeder et al., 2005; Reed, Weaver & Pomponi, 2006; Brooke & Schroeder, 2007; Lunden, Georgian & Cordes, 2013; Georgian et al., 2016a). While fossilized *Lophelia* rubble have been reported in the Colombian Caribbean (Santodomingo et al., 2007) and live *Lophelia* has been observed on the Brazilian continental margin (Arantes et al., 2009), the southern Caribbean (Hernández-Ávila, 2014), and off Roatan, Honduras (Henry, 2011), members of this genus have not been extensively reported in the insular Caribbean (OBIS, 2019).

We were also able to identify some variability in local distribution patterns among seamounts for three colonial scleractinian species. *Enallopsammia rostrata*, *Dendrophyllia alternata*, and *Solenosmilia variabilis* appear to have patchy distributions on the Anegada Passage seamounts. For example, only two colonies of *E. rostrata* were observed, both on Dog Seamount at 785m, and only five colonies of *D. alternata* were observed on Conrad Seamount between 490-598 m (Fig. 3). Similarly, *S. variabilis* was only observed in patches on Conrad Seamount from 490-569 m (Fig. 3). *Solenosmilia* has not been widely reported from the greater Caribbean basin based on records from the Ocean Biogeographic Information System (OBIS, 2019), but is known to be a contributor to coral mound formation off Brazil (Raddatz et al., 2020). *Solenosmilia* has been more commonly reported to asexually reproduce, and thus has a relatively short dispersal ability (Miller & Gunasekera, 2017), potentially explaining its patchy distribution.

Several coral taxa encountered in the Anegada Passage are important species for understanding biogeographic patterns of the Caribbean bathyal zone. *Madracis myriaster* was observed both on Dog and Conrad Seamounts, but only between 253 - 311 m. More recently, *M. myriaster* has been observed at similar depths and in high densities during surveys by the ROV



405

406

407

408

409

410

411

412

413

414

415

416

417

418

419

420

421

422

423

424

425

426

Deep Discoverer on the NOAA Ship Okeanos Explorer east of Viegues Island and in the Mona Passage at similar depths (Wagner et al., 2019). Northern and eastern Caribbean coral communities at continental shelf depths have been found to be dissimilar from the southern Caribbean, such that they may constitute distinct ecoregions (Hernández-Ávila, 2014). These differences were found to be driven by differences in the abundance of M. myriaster (Fig. 8C), which is more common at mesophotic and upper bathyal depths (Reyes et al., 2005; Santodomingo et al., 2007; Hernández-Ávila, 2014). At lower bathyal depths, regional biogeographic differences have also been attributed to variation in the frequency of solitary scleractinian species (e.g. Stephanocyathus sp., Fungiacyathus sp.) that may be difficult to detect during video transects (Hernández-Ávila, 2014). A greater diversity of solitary scleractinian corals and smaller stylasterids may have been present in the video but could not be documented due to limitations of ROV surveys (discussed in Everett & Park, 2018). The lack of easily identifiable diagnostic features from video, rugose terrain (e.g. overhangs and ledges), and rarity make most smaller species difficult to identify from ROV surveys without voucher specimens. A more thorough analysis incorporating modern (e.g. higher-resolution ROV video surveys with in situ collections) and historical datasets (e.g. museum-archived specimens) would be helpful in elucidating biogeographic patterns more broadly across the basin. Several species in the genus *Crypthelia* occur in the eastern Caribbean at bathyal depths (Cairns, 1986). The difficulty of identifying stylasterids from ROV video remains a challenge in establishing species occurrences, necessitating a voucher collection to confirm morphospecies identity. Nevertheless, the depth distribution, colony morphology, and coloration of *Stylaster* sp. 1, is consistent with Stylaster roseus (Pallas, 1766), a tropically-distributed western Atlantic stylasterid from depths typically less than 500 m (OBIS, 2019). Crypthelia sp. and other





stylasterid species are more likely to be underreported due to their small size (2-5 cm), on the threshold of being able to be accurately recorded from ROV video. These stylasterids were also observed under overhangs which made obtaining an accurate account of their abundance difficult. In this case, the reported occurrences of these corals represent a minimum value.

The ecological contribution of stylasterid corals is often understated, despite the ability of some species to produce significant three-dimensional structures that can act as habitat for other organisms. Larger structure-forming stylasterids are functionally analogous to some colonial scleractinian corals in that they can provide habitat for larger organisms such as deep-water fishes and invertebrates (Love, Lenarz & Snook, 2010; Braga-Henriques et al., 2011). *Crypthelia* spp., while relatively abundant in places and occurring over a wide range, were never observed above 12 cm in overall height and were observed to be extremely brittle when attempting collection (Fig. 9A). However, two species in the genus *Stylaster*, *S.* cf. *duchassaingi* (Fig. 9B) and *Stylaster* sp. 1 (Fig. 9C), can be classified as potentially important three-dimensional structure-forming species, primarily occurring between 150-400 m depth.

The carbonate mineralogy of most stylasterids is similar to scleractinians in that a majority of known species, including those observed in this study, produce a skeleton composed primarily of the mineral aragonite (Cairns, 2011), although some are calcitic in composition (Cairns & Macintyre, 1992). Stylasterids do share distribution characteristics and overlapping depth ranges with many upper bathyal solitary and colonial scleractinian corals (Cairns, 1986, 2011). Like scleractinians, stylasterid hydrocorals also exhibit a vulnerability to changing aragonite saturation conditions over their depth distribution (Guinotte et al., 2006).





450

451

452

453

454

455

456

457

458

459

460

461

462

463

464

465

466

467

468

469

470

471

significantly in recent years as empirical measurements of the carbonate system at deep-sea coral habitats have been reported from different regions across the global ocean. On seamounts in the Indian Ocean off the coast of SW Australia, the majority of framework-forming scleractinians – including E. rostrata and S. variabilis – were found at Ω_{arag} values at or just below saturation, suggesting a control on the lower limit of these species' distributions (Thresher et al., 2011). However, live scleractinian reefs were recently discovered on seamounts in the North Pacific at Ω_{arag} values as low as 0.71 (Baco et al., 2017) and as low as 0.81 off Southern California (Gómez et al., 2018). Additionally, scleractinians have been observed below the ASH in the Indian Ocean (Trotter et al., 2019) and South Atlantic Ocean (Barbosa, Davies & Sumida, 2020). These revelations indicate that, under the right conditions, scleractinian corals can persist in undersaturated waters (Baco et al., 2017). Additionally, the presence of live tissue may buffer against the effects of low pH (Venn et al., 2011), but the underlying dead coral framework may be less resilient to undersaturated waters. Expanded surveys below 2000 m in northern Caribbean, in tandem with additional effort in sampling of coral-adjacent deep-waters for carbonate chemistry analysis will aid in better determining the controls on aragonitic coral species distribution at lower bathyal depths in the tropical western Atlantic. Productivity of the surface waters and export to the deep-sea benthos may contribute to differences in species distribution and abundance of deep-sea corals. In a 2016 laboratory experiment and field study comparing two spatially distinct and genetically isolated populations of the framework-forming scleractinian Lophelia pertusa, colonies from Norway exhibited enhanced respiration and prey capture rates under acidified conditions compared to individuals

from the Gulf of Mexico (Georgian et al., 2016b). This study lends support to the hypothesis that

Knowledge of the chemical environment of deep-sea scleractinians has grown



species are locally adapted to environmental conditions, including food supply, which may allow individuals to better tolerate reduced carbonate saturation states.

Conclusions

474 475 476

477

478

479

480

481

482

483

484

485

486

487

488

489

490

491

492

493

494

472

473

Our results offer some insights to the distribution, diversity, and drivers of community assembly of scleractinian and stylasterid deep-water corals in a data-deficient region of the tropical western Atlantic Ocean. These findings lend support for the efficacy of targeted exploration surveys to understand coral distribution with respect to environmental gradients in the deep-sea environment. The presence of aragonitic corals, largely occurring above the aragonite saturation horizon, was not unexpected, but more surprising was the presence of known framework-forming scleractinians, like *Madrepora oculata*, living at or just above Ω_{arao} =1 in this locality. Future work should seek to expand upon coral community inventories for this area to include members of the Octocorallia and Antipatharia, particularly to refine the relationship between community assembly and water mass structure. Increased taxonomic effort is needed to better identify cryptic coral morphospecies from the deep-sea benthos, and particularly for those size classes below the identification threshold for ROV video surveys. In the Atlantic Ocean, deep-water coral ecosystem health is likely to be negatively impacted by environmental change by the end of the current century. Warming deep-waters (Gleckler et al., 2016), thermohaline driven deep-water acidification (Pérez et al., 2018), and low latitude deoxygenation in the Atlantic (Montes et al., 2016) are among the greatest threats facing deepwater framework-forming corals. The relationship between coral occurrences and environmental variables reported here establish a critical baseline for the detection of the effects of deep ocean change to seafloor communities, which is crucial to effective conservation.

495



496 497	Acknowledgements
498	We would like to thank the efforts of the science party, master, and crew of the E/V Nautilus on
499	Exploration of the Anegada Passage (NA052). We would like to extend a special thanks to the
500	Ocean Exploration Trust for their support. Taxonomic assistance in identifying voucher material
501	was provided by Stephen Cairns (NMNH) for scleractinian and stylasterid corals. We would also
502	like to thank Jason Chaytor, Alex Rogers, Iván Hernández-Ávila, and Nadia Santodomingo for
503	their feedback in the revision of this manuscript. Any use of trade, firm, or product names is for
504	descriptive purposes only and does not imply endorsement by the U.S. Government.
505	
506 507	References
508	Anderson M, Gorley RN, Clarke RK. 2008. Permanova+ for Primer: Guide to Software and
509	Statistical Methods. Primer-E Limited.
510	Arantes RCM, Castro CB, Pires DO, Seoane JCS. 2009. Depth and water mass zonation and
511	species associations of cold-water octocoral and stony coral communities in the
512	southwestern Atlantic. Marine Ecology Progress Series 397:71–79. DOI:
513	10.3354/meps08230.
514	Baco AR, Morgan N, Roark EB, Silva M, Shamberger KEF, Miller K. 2017. Defying
515	Dissolution: Discovery of Deep-Sea Scleractinian Coral Reefs in the North Pacific.
516	Scientific Reports 7:1–11. DOI: 10.1038/s41598-017-05492-w.
517	Barbosa R V, Davies AJ, Sumida PYG. 2020. Habitat suitability and environmental niche
518	comparison of cold-water coral species along the Brazilian continental margin. Deep Sea
519	Research Part I: Oceanographic Research Papers 155:103147.
520	Braga-Henriques A, Carreiro-Silva M, Porteiro FM, De Matos V, Sampaio Í, Ocaña O, Ávila SP



521	2011. The association between a deep-sea gastropod <i>Pedicularia sicula</i> (Caenogastropoda:
522	Pediculariidae) and its coral host Errina dabneyi (Hydrozoa: Stylasteridae) in the Azores.
523	ICES Journal of Marine Science 68:399-407. DOI: 10.1093/icesjms/fsq066.
524	Brooke S, Schroeder WW. 2007. State of deep coral ecosystems in the Gulf of Mexico region:
525	Texas to the Florida Straits. The State of Deep Coral Ecosystems of the United States:271-
526	306.
527	Cairns SD. 1979. The deep-water Scleractinia of the Caribbean Sea and adjacent waters. Studies
528	on the Fauna of Curação and other Caribbean Islands 57:1–341.
529	Cairns SD. 1986. A revision of the northwest Atlantic Stylasteridae (Coelenterata: Hydrozoa).
530	Smithsonian Contributions to Zoology:1– DOI: 10.5479/si.00810282.418.
531	Cairns SD. 2007. Deep-water corals: An overview with special reference to diversity and
532	distribution of deep-water scleractinian corals. In: Bulletin of Marine Science.
533	Cairns SD. 2011. Global diversity of the stylasteridae (Cnidaria: Hydrozoa: Athecatae). <i>PLoS</i>
534	ONE 6. D 10.1371/journal.pone.0021670.
535	Cairns SD, Chapman RE. 2001. Biogeographic affinities of the North Atlantic deep-water
536	Scleractinia. Proceedings of the First International Symposium on Deep-Sea Corals
537	Cairns SD, Macintyre IG. 1992. Phylogenetic implications of calcium carbonate mineralogy in
538	the Stylasteridae (Cnidaria: Hydrozoa). <i>Palaios</i> : 96–107.
539	Clarke KR, Gorley RN. 2006. User manual/tutorial. PRIMER-E Ltd., Plymouth.
540	Clarke KR, Somerfield PJ, Gorley RN. 2008. Testing of null hypotheses in exploratory
541	community analyses: similarity profiles and biota-environment linkage. Journal of
542	Experimental Marine Biology and Ecology 366:56–69. DOI: 10.1016/j.jembe.2008.07.009.
543	Cordes EE, Jones DOB, Schlacher TA, Amon DJ, Bernardino AF, Brooke S, Carney R, DeLeo



544	DM, Dunlop KM, Escobar-Briones EG, Gates AR, Genio L, Gobin J, Henry LA, Herrera S,
545	Hoyt S, Joye M, Kark S, Mestre NC, Metaxas A, Pfeifer S, Sink K, Sweetman AK, Witte U.
546	2016. Environmental impacts of the deep-water oil and gas industry: A review to guide
547	management strategies. Frontiers in Environmental Science 4. DOI:
548	10.3389/fenvs.2016.00058.
549	Davies AJ, Guinotte JM. 2011. Global habitat suitability for framework-forming cold-water
550	corals. PloS one 6:e18483.
551	Dickson AG, Sabine CL, Christian JR. 2007. Guide to best practices for ocean CO2
552	measurements. North Pacific Marine Science Organization.
553	https://www.oceanbestpractices.net/handle/11329/249
554	Everett M V., Park LK. 2018. Exploring deep-water coral communities using environmental
555	DNA. Deep Sea Research Part II: Topical Studies in Oceanography 150:229–241. DOI:
556	10.1016/J.DSR2.2017.09.008.
557	Georgian SE, DeLeo D, Durkin A, Gomez CE, Kurman M, Lunden JJ, Cordes EE. 2016a.
558	Oceanographic patterns and carbonate chemistry in the vicinity of cold-water coral reefs in
559	the Gulf of Mexico: Implications for resilience in a changing ocean. Limnology and
560	Oceanography 61:648–665.
561	Georgian SE, Dupont S, Kurman M, Butler A, Strömberg SM, Larsson AI, Cordes EE. 2016b.
562	Biogeographic variability in the physiological response of the cold-water coral Lophelia
563	pertusa to ocean acidification. Marine Ecology 37:1345–1359. DOI: 10.1111/maec.12373.
564	Georgian SE, Shedd W, Cordes EE. 2014. High-resolution ecological niche modelling of the
565	cold-water coral Lophelia pertusa in the Gulf of Mexico. Marine Ecology Progress Series
566	506:145–161. DOI: 10.3354/meps10816.



567	Gleckler PJ, Durack PJ, Stouffer RJ, Johnson GC, Forest CE. 2016. Industrial-era global ocean
568	heat uptake doubles in recent decades. <i>Nature Climate Change</i> 6:394–398. DOI:
569	10.1038/nclimate2915.
570	Gómez CE, Wickes L, Deegan D, Etnoyer PJ, Cordes EE. 2018. Growth and feeding of deep-sea
571	coral Lophelia pertusa from the California margin under simulated ocean acidification
572	conditions. <i>PeerJ</i> 2018. I : 10.7717/peerj.5671.
573	Guinotte JM, Orr J, Cairns S, Freiwald A, Morgan L, George R. 2006. Will human-induced
574	changes in seawater chemistry alter the distribution of deep-sea scleractinian corals?
575	Frontiers in Ecology and the Environment 4:141–146.
576	Henry LA. 2011. A deep-sea coral 'gateway' in the northwestern Caribbean. <i>Palomares MLD</i> ,
577	Pauly D Too Precious to Drill: the Marine Biodiversity of Belize:120–124.
578	Hernández-Ávila I. 2014. Patterns of deep-water coral diversity in the Caribbean basin and
579	adjacent southern waters: An approach based on records from the R/V Pillsbury
580	expeditions. PLoS ONE 9. DOI: 10-1371/journal.pone.0092834.
581	Huang W, Wang Y, Cai W. 2012. Assessment of sample storage techniques for total alkalinity
582	and dissolved inorganic carbon in seawater. Limnology and oceanography: Methods
583	10:711–717.
584	Jiang L, Feely RA, Carter BR, Greeley DJ, Gledhill DK, Arzayus KM. 2015. Climatological
585	distribution of aragonite saturation state in the global oceans. Global Biogeochemical
586	Cycles 29:1656–1673. DOI: 10.1002/2015GB005198.
587	Littler MM, Littler DS, Blair SM, Norris JN. 1986. Deep-water plant communities from an
588	uncharted seamount off San Salvador Island, Bahamas: distribution, abundance, and primary
589	productivity. Deep-sea Research 33:881–892.



590	Liu M, Tanhua T. 2019. Distribution of Water Masses in the Atlantic Ocean based on
591	GLODAPv2. Ocean Science Discussions:1–32. DOI: 10.5194/os-2018-140.
592	Love MS, Lenarz B, Snook L. 2010. A survey of the reef fishes, purple hydrocoral (Stylaster
593	californicus), and marine debris of Farnsworth Bank, Santa Catalina Island. Bulletin of
594	Marine Science 86:35–52.
595	Lunden JJ, Georgian SE, Cordes EE. 2013. Aragonite saturation states at cold-water coral reefs
596	structured by Lophelia pertusa in the northern Gulf of Mexico. Limnology and
597	Oceanography 58:354–362. DOI: 10.4319/lo.2013.58.1.0354.
598	Lutz SJ, Ginsburg RN. 2007. State of deep coral ecosystems in the Caribbean region: Puerto
599	Rico and the US Virgin Islands. The State of Deep Coral Ecosystems of the United States.
600	NOAA Technical Memorandum CRCP-3, Silver Spring, MD:307-365.
601	Messing CG, Neumann AC, Lang JC. 1990. Biozonation of Deep-Water Lithoherms and
602	Associated Hardgrounds in the Northeastern Straits of Florida. <i>Palaios</i> 5:15–33.
603	Miller KJ, Gunasekera RM. 2017. A comparison of genetic connectivity in two deep sea corals
604	to examine whether seamounts are isolated islands or stepping stones for dispersal.
605	Scientific Reports 7:1–14. DOI: 10.1038/srep46103.
606	Miller KA, Thompson KF, Johnston P, Santillo D. 2018. An Overview of Seabed Mining
607	Including the Current State of Development, Environmental Impacts, and Knowledge Gaps.
608	Frontiers in Marine Science 4:418. DOI: 10.3389/fmars.2017.00418.
609	Miloslavich P, Díaz JM, Klein E, Alvarado JJ, Díaz C, Gobin J, Escobar-Briones E, Cruz-Motta
610	JJ, Weil E, Cortés J, Bastidas AC, Robertson R, Zapata F, Martín A, Castillo J, Kazandjian
611	A, Ortiz M. 2010. Marine biodiversity in the caribbean: Regional estimates and distribution
612	patterns. PLoS ONE 5. T: 10.1371/journal.pone.0011916.



613	Montes E, Muller-karger FE, Cianca A, Lomas MW, Lorenzoni L, Habtes S. 2016. Decadal
614	variability in the oxygen inventory of North Atlantic subtropical underwater captured by
615	sustained, long-term oceanographic time series observations. Global Biogeochemical Cycles
616	30:460–478. DOI: 10.1002/2015GB005183.Received.
617	Morrison JM, Nowlin WD. 1982. General distribution of water masses within the eastern
618	Caribbean Sea during the winter of 1972 and fall of 1973. Journal of Geophysical
619	Research: Oceans 87:4207–4229.
620	OBIS. 2019. Ocean Biogeographic Information System. Intergovernmental Oceanographic
621	Commission of UNESCO.
622	Pérez FF, Fontela M, Garcia-Ibañez MI, Mercier H, Velo A, Lherminier P, Zunino P, de la Paz
623	M, Alonso-Pérez F, Guallart EF, Padin XA. 2018. Meridional overturning circulation
624	conveys fast acidification to the deep Atlantic Ocean. <i>Nature</i> . Len: 10.1038/nature25493.
625	Quattrini AM, Demopoulos AWJ, Singer R, Roa-Varon A, Chaytor JD. 2017. Demersal fish
626	assemblages on seamounts and other rugged features in the northeastern Caribbean. Deep
627	Sea Research Part I: Oceanographic Research Papers. DOI: 10.1016/j.dsr.2017.03.009.
628	Raddatz J, Titschack J, Frank N, Freiwald A, Conforti A, Osborne A, Skornitzke S, Stiller W,
629	Rüggeberg A, Voigt S, Albuquerque ALS, Vertino A, Schröder-Ritzrau A, Bahr A. 2020.
630	Solenosmilia variabilis-bearing cold-water coral mounds off Brazil. Coral Reefs 39:69-83.
631	DOI: 10.1007/s00338-019-01882-w.
632	Ragnarsson SÁ, Burgos JM, Kutti T, Beld I Van Den, Egilsdóttir H, Arnaud-haond S, Grehan A.
633	2017. The impact of Anthropogenic Activity on Cold-Water Corals. In: Rossi S ed. Marine
634	Animal Forests. Springer International Publishing, 1–35. DOI: 10.1007/978-3-319-17001-5.
635	Reed JK, Messing C, Walker BK, Brooke S, Correa TBS, Brouwer M, Udouj T, Farrington S.



636	2013. Habitat Characterization, Distribution, and Areal Extent of Deep-sea Coral
637	Ecosystems off Florida, Southeastern U.S.A. Caribbean Journal of Science 47:13–30. DOI:
638	10.18475/cjos.v47i1.a3.
639	Reed JK, Weaver DC, Pomponi SA. 2006. Habitat and fauna of deep-water Lophelia pertusa
640	coral reefs off the southeastern US: Blake Plateau, Straits of Florida, and Gulf of Mexico.
641	Bulletin of Marine Science 78:343–375.
642	Reyes J, Santodomingo N, Gracia A, Borrero-Pérez G, Navas G, Mejía-Ladino LM, Bermúdez
643	A, Benavides M. 2005. Southern Caribbean azooxanthellate coral communities off
644	Colombia. In: Cold-water corals and Ecosystems. Springer, 309–330.
645	Robbins LL, Hansen ME, Kleypas JA, Meylan SC. 2010. CO2calc: A user-friendly seawater
646	carbon calculator for Windows, Mac OS X, and iOS (iPhone). US Geological Survey.
647	Roberts JM, Wheeler A, Freiwald A, Cairns SD. 2009. Cold-water corals: the biology and
648	geology of deep-sea coral habitats. Cambridge University Press.
649	Rogers AD. 1994. The biology of seamounts. In: Advances in marine biology. Elsevier, 305-
650	350.
651	Rogers AD. 2018. The Biology of Seamounts: 25 Years on. Advances in Marine Biology
652	79:137–224. DOI: 10.1016/BS.AMB.2018.06.001.
653	Santodomingo N, Reyes J, Gracia A, Martínez A, Ojeda G, García C. 2007. Azooxanthellate
654	Madracis coral communities off San Bernardo and Rosario Islands (Colombian Caribbean).
655	Bulletin of Marine Science 81:273–287.
656	Schlitzer R. 2019. Ocean data view. Available at: https://odv.awi.de/
657	Schroeder WW, Brooke SD, Olson JB, Phaneuf B, McDonough JJ, Etnoyer P. 2005. Occurrence
658	of deep-water Lophelia pertusa and Madrepora oculata in the Gulf of Mexico. In: Cold-

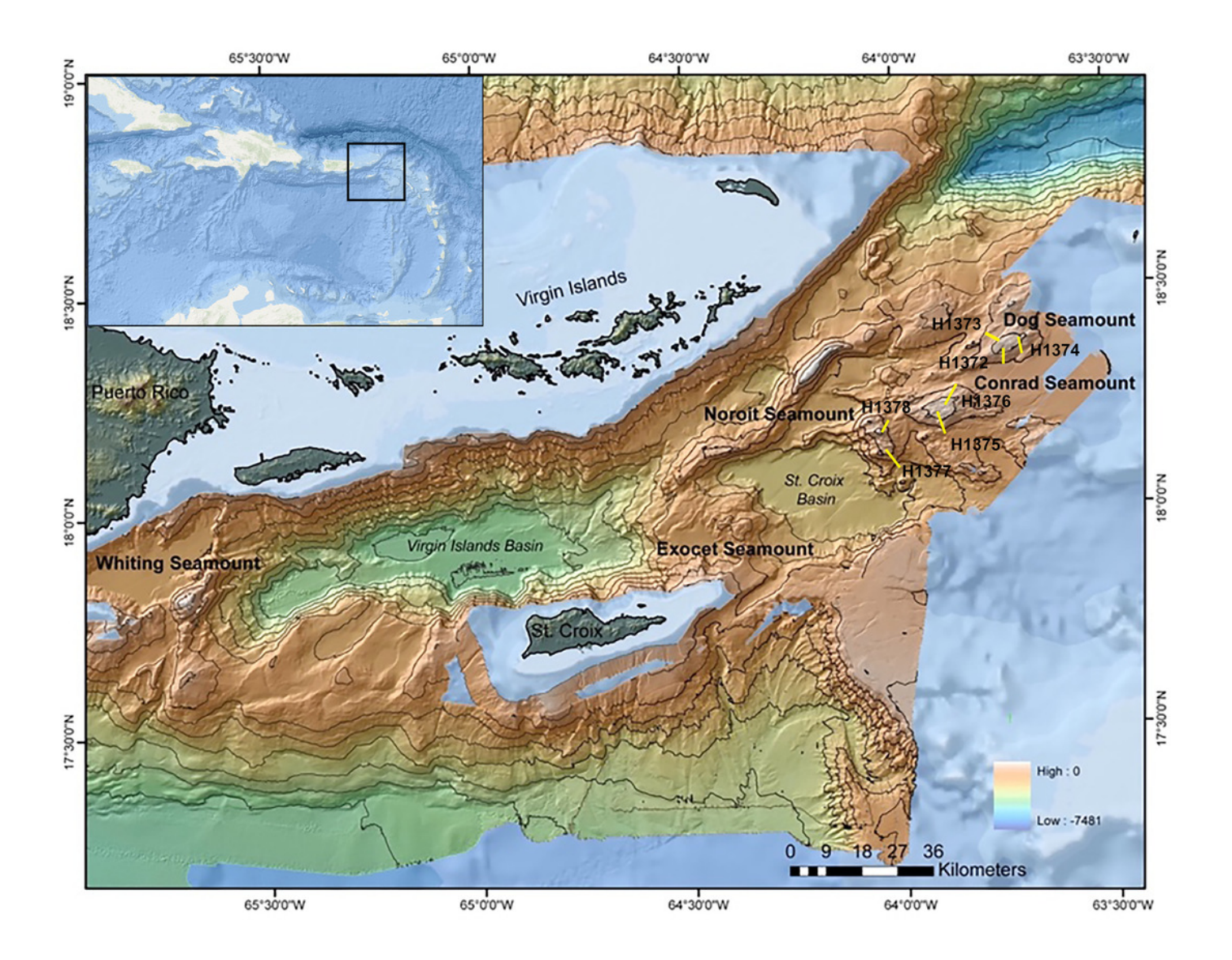




659	water corals and ecosystems. Springer, 297–307.
660	Thresher RE, Tilbrook B, Fallon S, Wilson NC, Adkins J. 2011. Effects of chronic low carbonate
661	saturation levels on the distribution, growth and skeletal chemistry of deep-sea corals and
662	other seamount megabenthos. Marine Ecology Progress Series 442:87–99. DOI:
663	10.3354/meps09400.
664	Trotter JA, Pattiaratchi C, Montagna P, Taviani M, Falter J, Thresher R, Hosie A, Haig D,
665	Foglini F, Hua Q. 2019. First ROV exploration of the Perth Canyon: Canyon setting, faunal
666	observations, and anthropogenic impacts. Frontiers in Marine Science.
667	Venn A, Tambutté E, Holcomb M, Allemand D, Tambutté S. 2011. Live tissue imaging shows
668	reef corals elevate pH under their calcifying tissue relative to seawater. <i>PLoS ONE</i> 6. DOI:
669	10.1371/journal.pone.0020013.
670	Wagner D, Sowers D, Williams SM, Auscavitch S, Blaney D, Cromwell M. 2019. Océano
671	Profundo 2018: Exploring deep sea <mark>habitats off Puerto Rico and the US Virgin Islands. = = = = = = = = = = = = = = = = = = </mark>
672	Watling L, Norse EA. 1998. Disturbance of the Seabed by Mobile Fishing Gear: A Comparison
673	to Forest Clearcutting. Conservation Biology 12:1180–1197.
674	
675	
676	

Multibeam bathymetric map of the Anegada Passage seamounts.

The locations of Dog, Conrad, and Noroît Seamount are indicated in bold. Dive locations are overlaid in yellow and labeled by dive number. The bathymetry color ramp in the lower right indicates depth values measured in meters. Transect segments lengths are not drawn to scale.

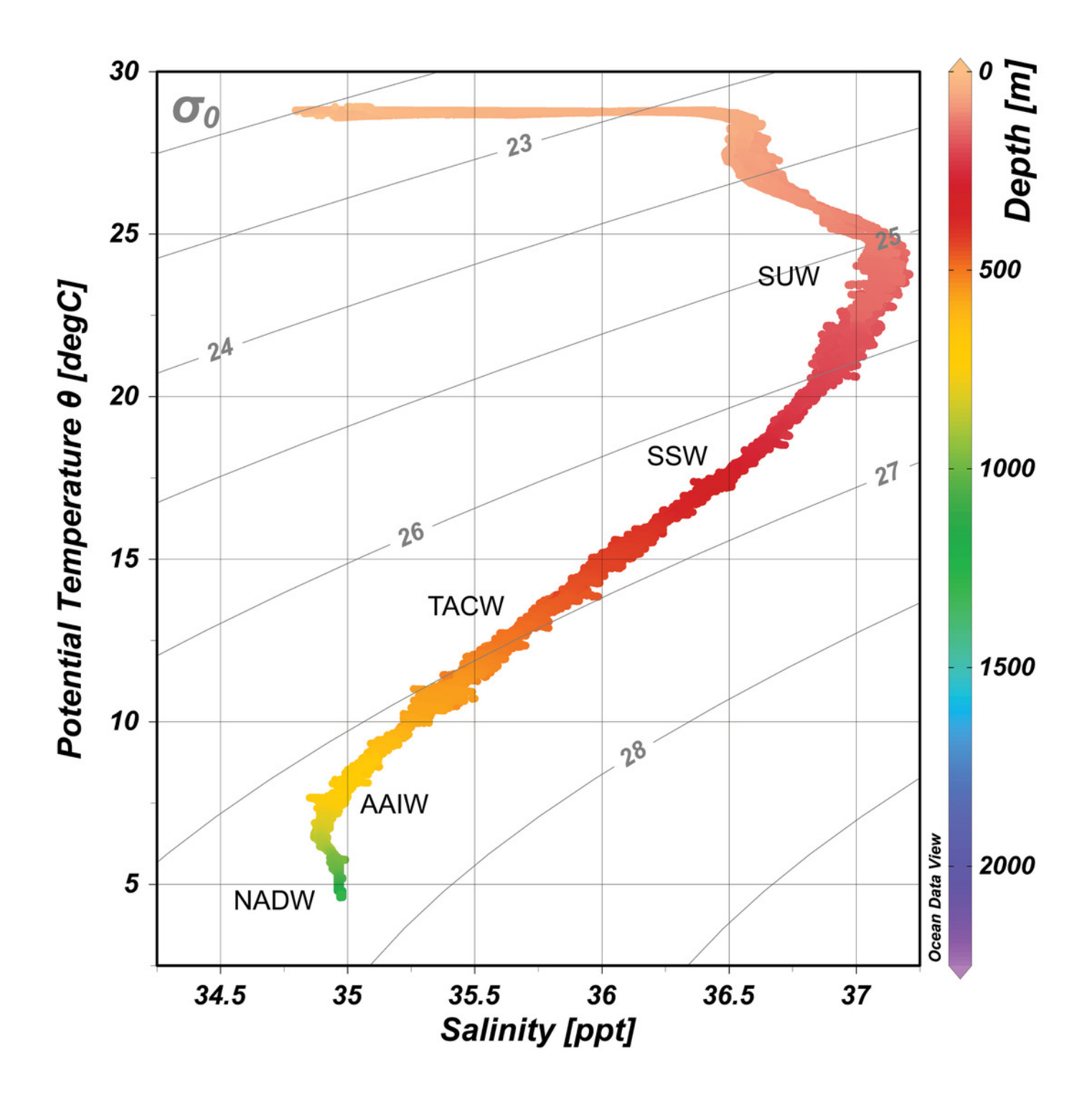




Temperature-Salinity plot for the Anegada Passage based on CTD water column profiles.

Water masses are overlaid and abbreviated by the following: SUW=Subtropical underwater, SSW=Sargasso Sea Water, TACW= Tropical Atlantic Central Water, AAIW=Antarctic Intermediate Water, and NADW=North Atlantic Deep Water. Isopycnal surfaces (σ_{θ}) are indicated in gray.

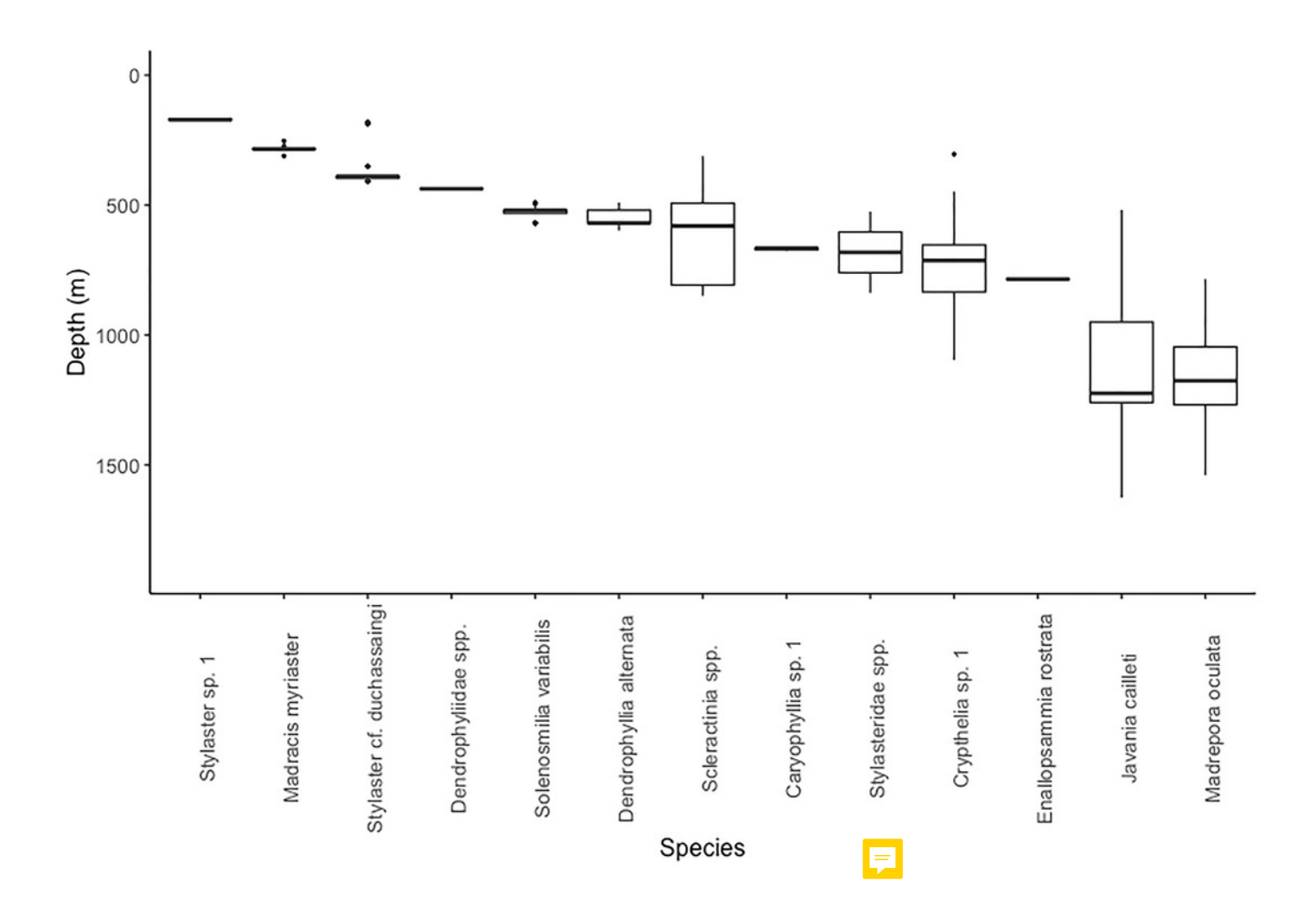






Depth distribution for scleractinian and stylasterid corals occurring on Dog, Conrad, and Noroît Seamounts.

Box plots represent the interquartile range with whiskers extending from the upper and lower quartiles to the minimum and maximum values. Horizontal lines represent the median depth. Individual points represent outliers. Species are arranged on the x-axis from shallowest to deepest by median depth of occurrence.

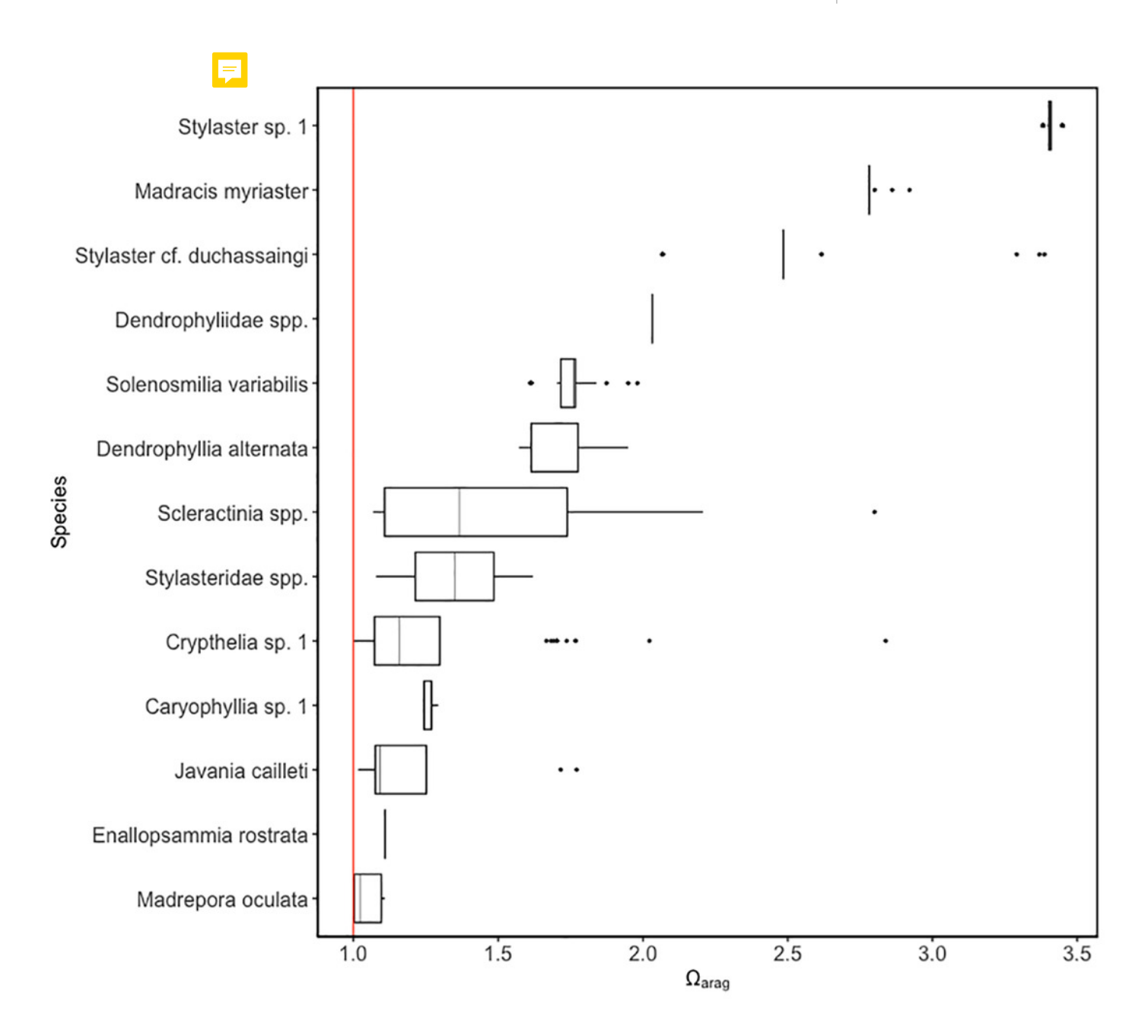




Distribution of scleractinian and stylasterid species against model predicted Ω_{Arag} values on the Anegada Passage seamounts.

Box plots represent the interquartile range with whiskers extending from the upper and lower quartiles to the minimum and maximum values. Vertical lines represent the median aragonite saturation state. Individual points represent outliers. Species are arranged on the y-axis from highest to lowest median aragonite saturation occurrence. A solid red vertical line indicates the aragonite saturation horizon, where $\Omega_{Arag} = 1$.

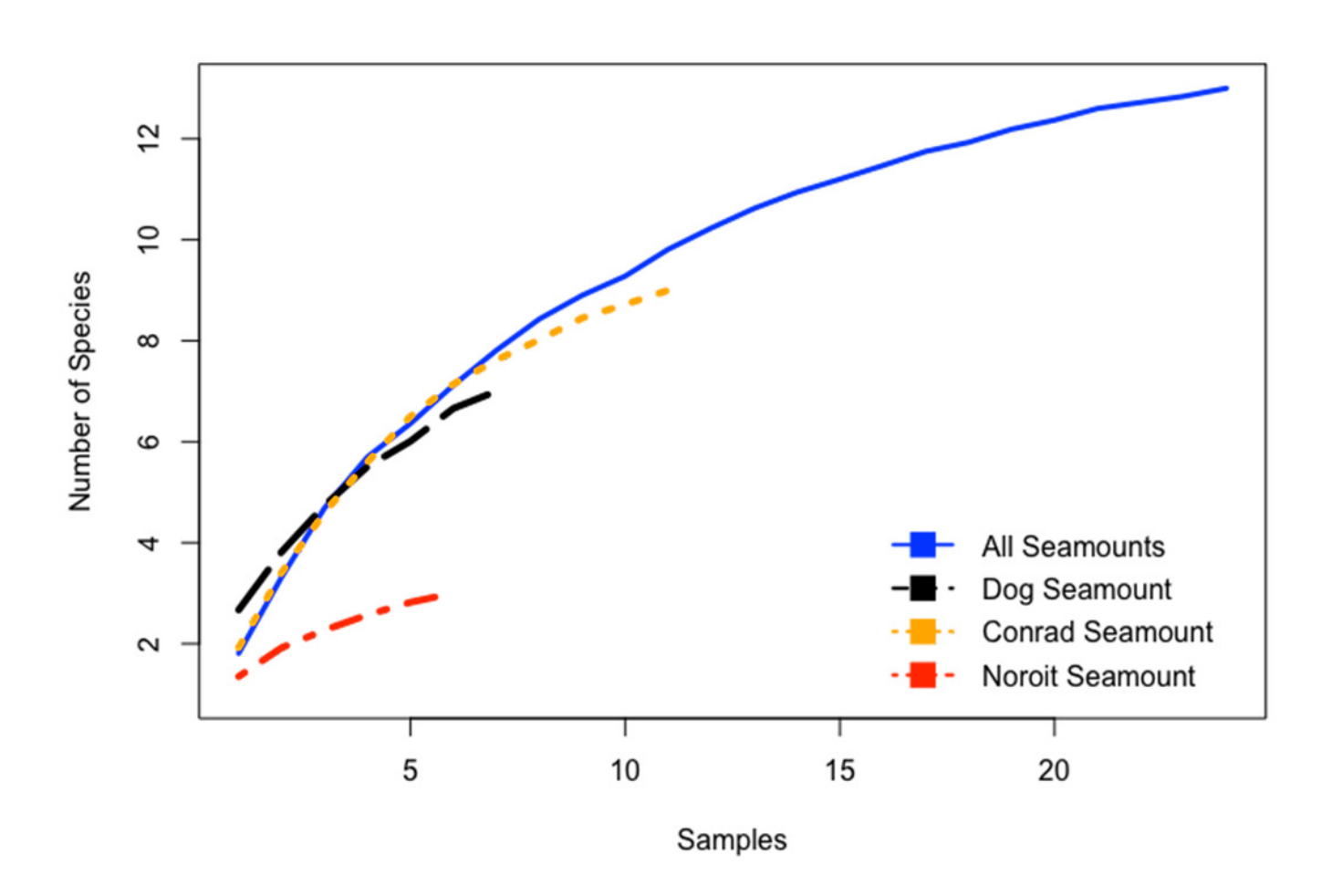






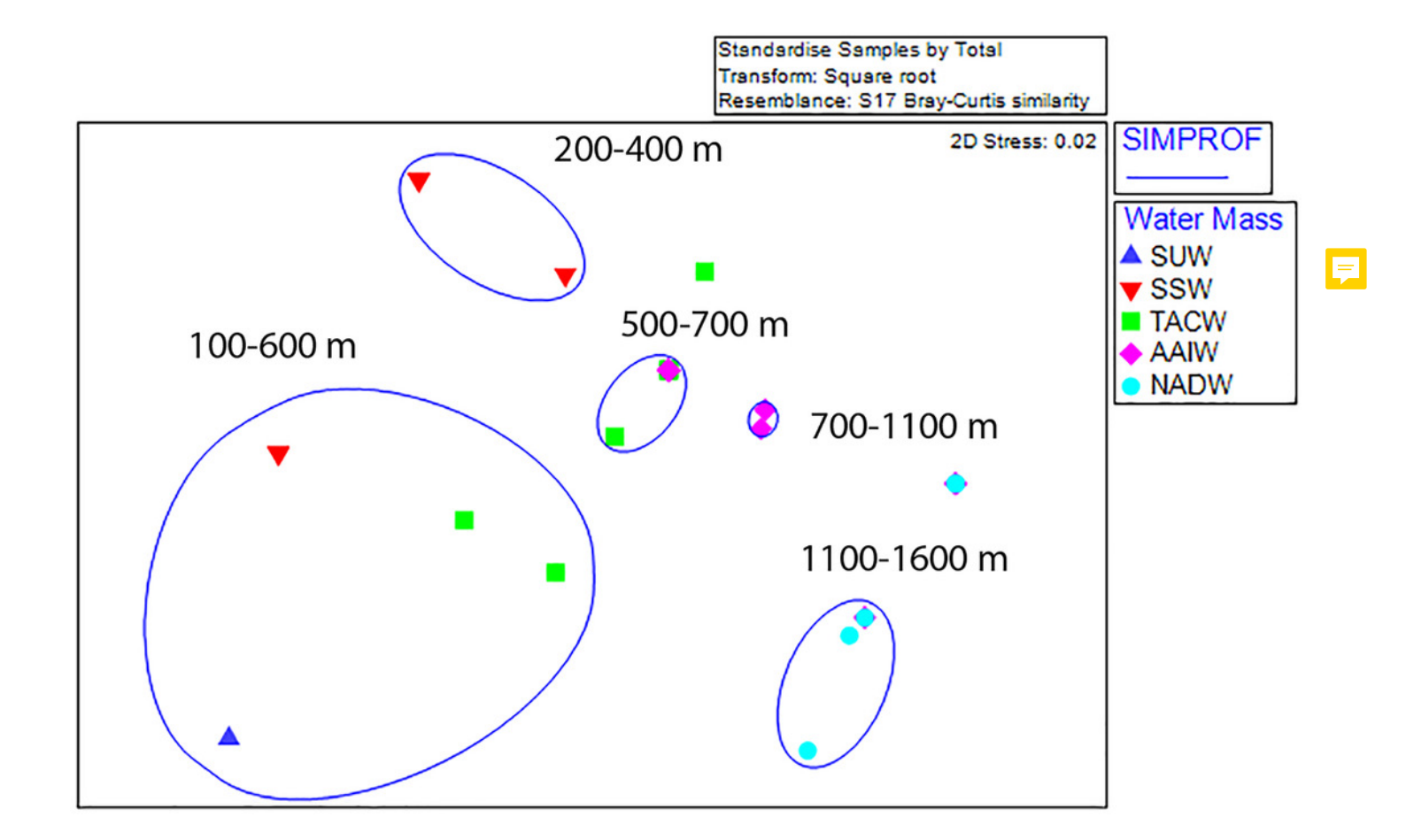
Species accumulation curves for the Anegada Passage seamounts.

Curves are plotted for all transects on Dog Seamount (276-1035 m), Conrad Seamount (162-1267 m), Noroit Seamount (881-2157 m), as well as for all three seamounts combined (162-2157 m).



Non-metric multidimensional scaling analysis of standardized, fourth-root transformed coral assemblages on Dog, Conrad, and Noroît Seamounts.

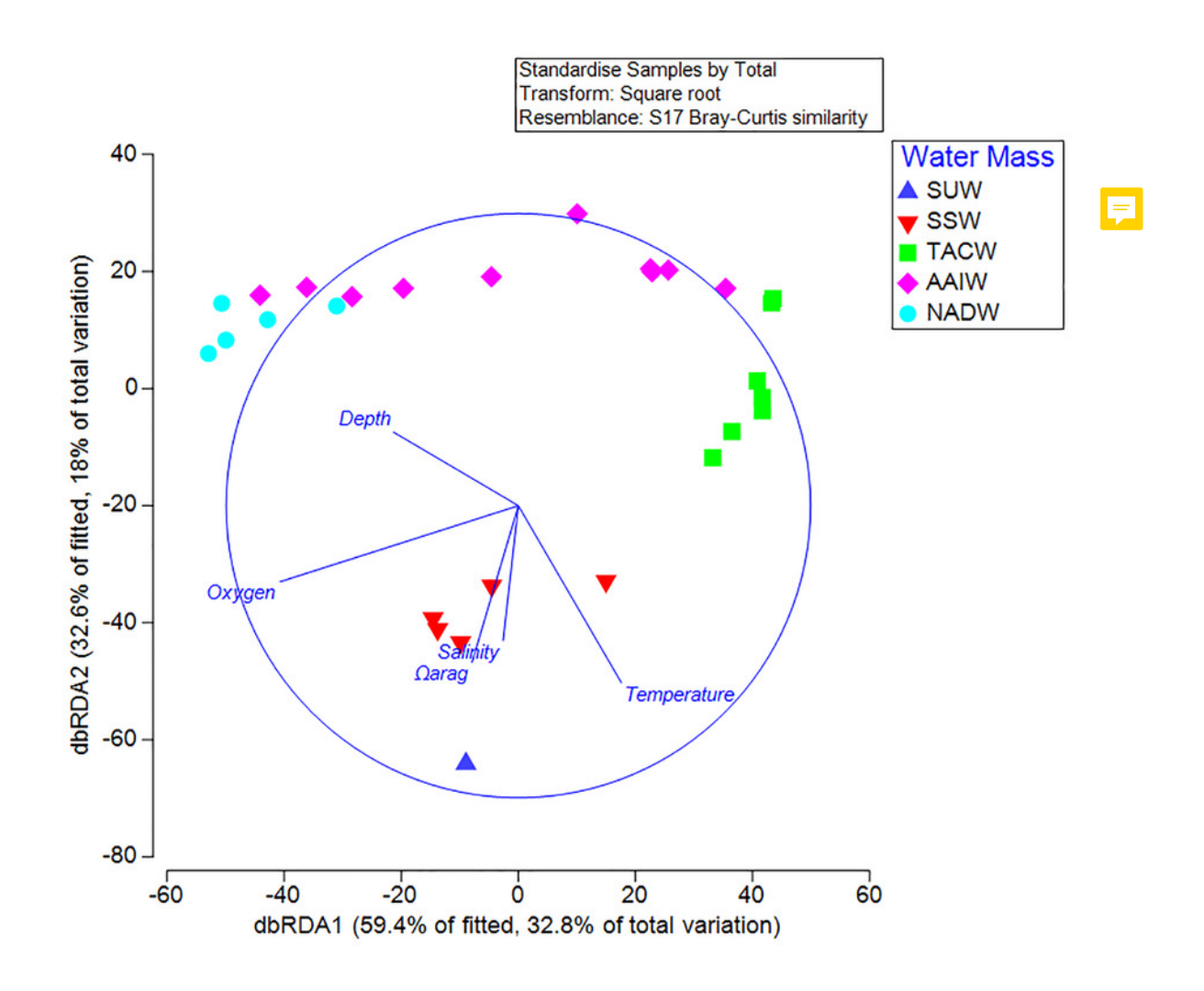
SIMPROF groups are overlaid around significant groupings at the 95% level or above. Depth ranges displayed within each statistical grouping are indicated in black text.





Distance-based linear model and redundancy analysis of coral assemblages and oceanographic variables.

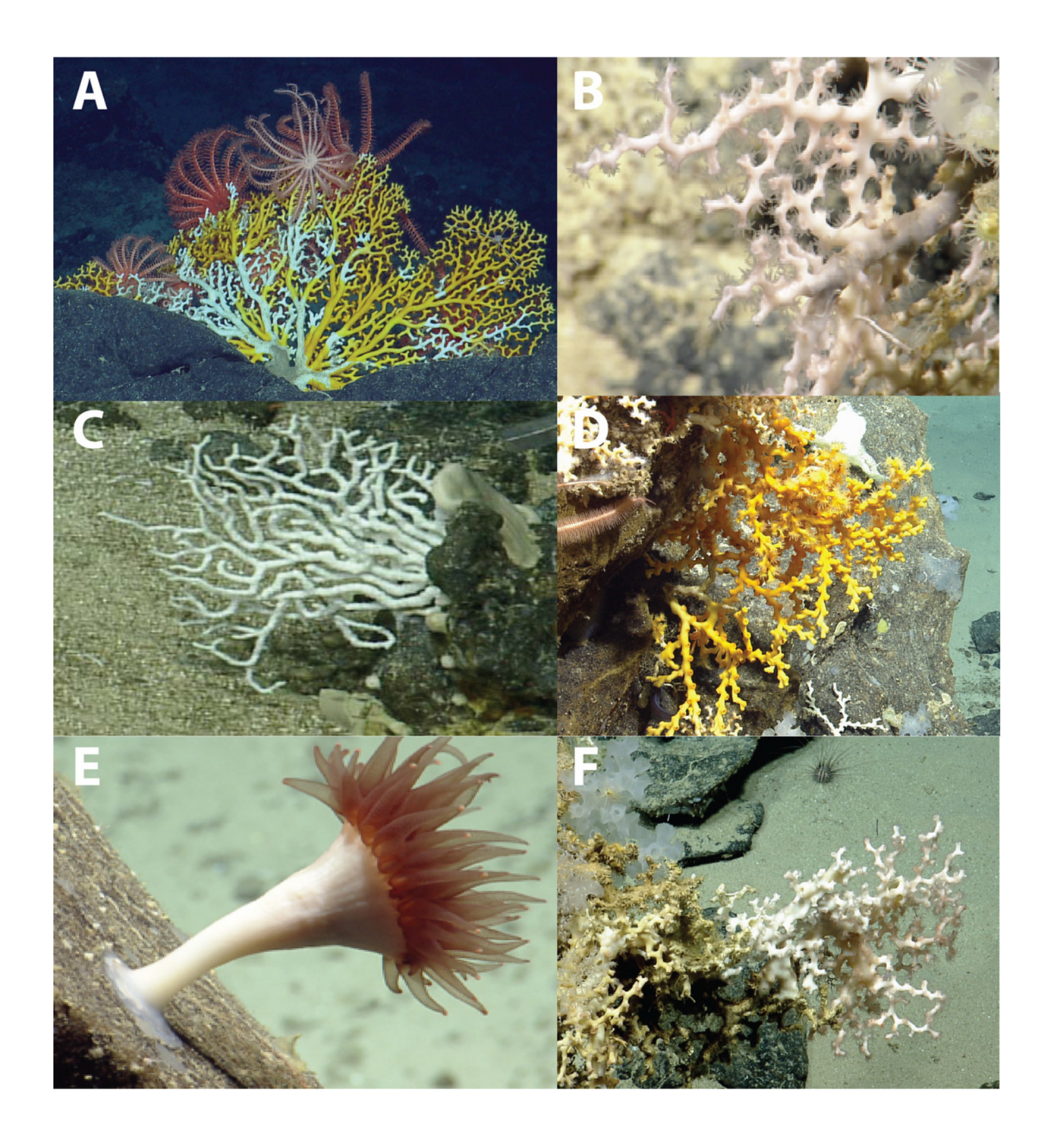
Sample points represent one 100 m depth assemblage. Axes shown are the results of a distance-based redundancy analysis with percent variation explained by the first and second axes.





Deep-water scleractinians from the Anegada Passage seamounts.

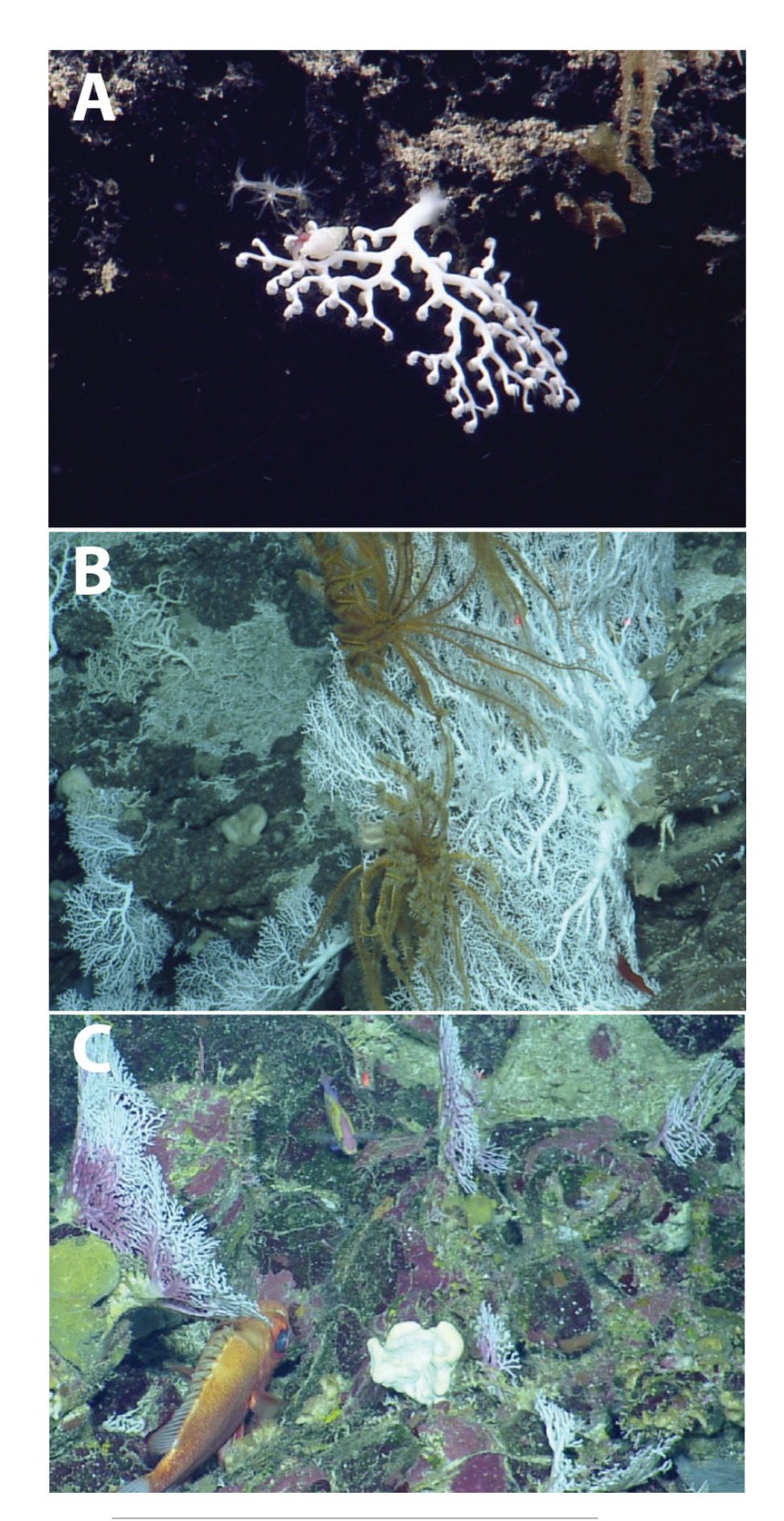
(A) Enallopsammia rostrata. (B) Madrepora oculata. (C) Madracis myriaster. (D) Dendrophyllia alternata. (E) Javania cailleti. (F) Solenosmilia variabilis.





Deep-water stylasterids from the Anegada Passage seamounts.

(A) Crypthelia sp. 1. (B) Stylaster cf. duchassaingi. (C) Stylaster sp. 1.



PeerJ reviewing PDF | (2018:04:27834:1:1:NEW 30 Apr 2020)



Table 1(on next page)

ROV dive transect details for 2014 surveys of the Anegada Passage seamounts.

Start and end coordinates for each transect, time spent in visual contact with the seafloor, and number of water samples collected at depth over the dive interval are indicated.



- 1 Table 1: ROV dive transect details for 2014 surveys of the Anegada Passage seamounts. Start
- 2 and end coordinates for each transect, time spent in visual contact with the seafloor, and number
- 3 of water samples collected at depth over the dive interval are indicated.

Dive	Seam ount	Start Coordinates	End Coordinates	Depth Range (m)	Number of Niskin Bottle Samples	Total Bottom Time (hh:mm)
H137 2	Dog	18°18.7385 N 63°46.0896 W	18°19.6177 N 63°46.1645 W	717-1035	6	07:56
H137 3	Dog	18°22.6480 N 63°46.1953 W	18°21.9711 N 63°45.9306 W	503-784	6	11:09
H137 4	Dog	18°20.4464 N 63°43.6091 W	18°21.9311 N 63°43.5024 W	276-601	5	09:58
H137 5	Conra d	18°10.5420 N 63°53.1020 W	18°13.0029 N 63°53.3459 W	162-876	5	31:40
H137 6	Conra d	18°16.4904 N 63°52.3364 W	18°14.2223 N 63°52.9767 W	344-1267	6	22:38
H137 7	Noroît	18° 05.4657 N 64° 00.1741 W	18° 07.0695 N 64° 01.1760 W	881-2157	6	17:10
H137 8	Noroît	18° 09.6969 N 64° 01.3606 W	18° 09.4122 N 64° 01.8888 W	949-1035	2	06:01



Table 2(on next page)

Summary of records and environmental variables for each taxon.

Ranges of values for number of observations, depth, temperature, salinity, dissolved oxygen, model predicted Ω_{Arag} , and colony height are reported for each species by taxonomic grouping.

- 1 Table 2: Summary of records and environmental variables for each taxon. Ranges of values for number of observations, depth,
- $2\quad \text{temperature, salinity, dissolved oxygen, model predicted } \Omega_{Arag} \text{ , and colony height are reported for each species by taxonomic}$
- 3 grouping.

Class	Family	Species	Number of observations	Depth (m)	Temperature (°C)	Salinity (psu)	Dissolved oxygen (mg/L)	Model Predicted Ω_{arag}	Height (cm)
Hydrozoa	Stylasteridae	Stylaster sp. 1	65	166-174	22.1-22.5	37.00-37.05	7-7.12	3.38-3.45	-
		Crypthelia sp. 1	49	304-1096	4.9-18.0	34.53-36.55	2.41-7.22	0.99-2.83	1-12
		Stylaster cf. duchassaingi	30	181-408	13.8-22.1	35.82-37.01	5.39-6.99	2.07-3.39	12-37
		Stylasteridae spp.	2	525-838	6.7-10.9	34.89-35.39	4.96-5.28	1.08-1.62	3-5
	Caryophylliidae	Solenosmilia variabilis	44	490-569	10.9-13.3	35.37-35.75	4.88-5.15	1.61-1.98	12-18
		Caryophyllia sp. 1	3	665-677	8.2-8.7	35.03-35.07	4.78-4.86	1.24-1.29	-
	Oculinidae	Madrepora oculata	22	784-1540	4.3-6.9	34.53-34.97	5.22-8.23	1.00-1.10	10-125
	Pocilloporidae	Madracis myriaster	22	253-311	17.6-18.7	36.49-36.65	6.83-7.01	2.78-2.92	6-35
	Incertae familiae	Scleractinia spp. (solitary)	11	311-849	6.5-17.8	34.83-36.51	4.76-6.98	1.07-2.8	4-5
	Dendrophylliidae	Dendrophyllia alternata	5	490-598	10.7-13	35.33-35.71	4.84-5.13	1.57-1.95	16
		Enallopsammia rostrata	2	785	7.0	34.921	5.2	1.11	20-75
		Dendrophylliidae spp.	1	437	13.6	35.794	5.29	2.03	5
	Flabellidae	Javania cailleti	8	518-1626	4.2-12.0	34.557-35.54	4.96-8.34	1.02-1.77	4-7



Table 3(on next page)

Summary of measured values of $\Omega_{\mbox{\tiny Arag}}$ from water samples taken directly adjacent to corals.

Sampling events are reported for each species arranged by taxonomic grouping.



- 1 Table 3: Summary of measured values of Ω_{Arag} from water samples taken directly adjacent to
- 2 corals. Sampling events are reported for each species arranged by taxonomic grouping.

Class	Family	Species	Number of adjacent water samples	Ω _{arag} measured
	Stylasteridae	Stylaster sp. 1	0	-
		Crypthelia sp. 1	0	-
Hydrozoa		Stylaster cf. duchassaingi	0	-
		Stylasteridae spp.	0	-
	Caryophylliidae	Solenosmilia variabilis	1	1.63
		Caryophyllia sp. 1	1	1.24
	Oculinidae	Madrepora oculata	2	1.13-1.16
	Pocilloporidae	Madracis myriaster	1	2.7
	Incertae familiae	Scleractinia spp. (solitary)	0	-
Anthozoa		Dendrophyllia alternata	1	1.35
	Dendrophylliidae	Enallopsammia rostrata	1	1.21
		Dendrophylliidae spp.	1	1.82
	Flabellidae	Javania cailleti	1	1.16